Entanglement Spectrum of a Disordered Topological Chern Insulator

Emil Prodan,[1] Taylor L. Hughes,[2] and B. Andrei Bernevig[3]

[1]*Department of Physics, Yeshiva University, New York, New York 10016, USA*
[2]*Department of Physics, University of Illinois, 1110 West Green Street, Urbana Illinois 61801, USA*
[3]*Department of Physics, Princeton University, Princeton, New Jersey 08544, USA*

(Received 27 May 2010; revised manuscript received 23 June 2010; published 7 September 2010)

We investigate the behavior of a topological Chern insulator in the presence of disorder, with a focus on its entanglement spectrum (EtS) constructed from the ground state. For systems with symmetries, the EtS was shown to contain explicit information about the topological universality class revealed by sorting the EtS against the conserved quantum numbers. In the absence of any symmetry, we demonstrate that statistical methods such as the level statistics of the EtS can be equally insightful, allowing us to distinguish when an insulator is in a topological or trivial phase and to map the boundary between the two phases. The phase diagram of a Chern insulator is explicitly computed as function of Fermi level (E_F) and disorder strength using the level statistics of the EtS and energy spectrum, together with a computation of the Chern number (C) via a new, efficient real-space formula.

DOI: 10.1103/PhysRevLett.105.115501 PACS numbers: 63.22.−m, 63.20.Pw

Topological insulators (TI) are materials that do not conduct electricity in the bulk but display conducting edge channels. Chern insulators (CIs) represent a particular class of TIs [1] that have broken time-reversal symmetry. They have not been observed yet experimentally, but a time-reversal invariant version has been proposed [2–4] and discovered [5]. Since then, the field of TIs became increasingly popular. The central claim of the field, and the basis for most potential applications, is the robustness of TIs' properties against imperfections. Our Letter contributes to the ongoing research [6–11] on disorder effects in TIs and gives two practical tests to determine if the ground state of a disordered CI is in the topological or trivial phase. The tests involve only the ground-state wave function.

While our work concentrates on CIs, it addresses a broader question: Given the ground state of a Hamiltonian, how much information can we extract about its "topological" universality class? Reference [12] suggested that the answer resides in the *entanglement spectrum*, i.e., the full set of eigenvalues of the reduced density matrix. For the $\nu = \frac{5}{2}$ fractional quantum hall states, the entanglement spectrum (EtS) levels and their multiplicities, when plotted versus the angular momentum, match the levels and multiplicities of the edge modes [12–14]. The EtS also captures the low-energy physics of gapless spin chains [15] and for topological insulators it exhibits analogs of the physical edge state spectra [16–19].

Prior studies on EtS treated systems with translational invariance and the EtS of fractional quantum hall states, spin chains, and topological insulators were plotted versus the momentum parallel to the cut. This is not generic and until now it was unclear if the EtS is useful when no symmetry is present. Without translational symmetry, what remains that is fundamental? Seminal thinking by Wigner gave us the answer: adopt a statistical view of spectra. Subsequent work on random matrix theory revealed universal spectral properties that are dependent only on the fundamental symmetries of the Hamiltonians [20]. This line of thinking has had success in both many-body systems as well as in the theory of Anderson localization. We adopt it here and apply it to the EtS rather than to the energy spectrum (EnS). For disordered CIs, we show that the EtS gives clear signatures of whether the CI is in the topologically nontrivial or in the simple Anderson-insulator state. Such signatures, present in the ground state alone, are important for developing tools to attack the interacting many-body problem with disorder since statistical analysis of the EnS is impossible for large systems—diagonalization procedures only give a few low-lying energy states. The EtS of the ground-state, however, contains a large number of eigenvalues on which level statistics can be performed. We compare our results for the EtS with computations of the Chern number via a real-space formula and with results from conventional level statistics of EnS.

We consider 2D lattice models with $\alpha = 1, \ldots, K$ quantum states $|\boldsymbol{x}, \alpha\rangle$ per each site $\boldsymbol{x}$ and Hamiltonians:

$$H_\omega = \sum t_{\alpha\beta}^{\boldsymbol{x}-\boldsymbol{y}} |\boldsymbol{x}, \alpha\rangle\langle \boldsymbol{y}, \beta| + W \sum \omega_{\boldsymbol{x},\alpha} |\boldsymbol{x}, \alpha\rangle\langle \boldsymbol{x}, \alpha|,$$

where the first term is a translationally invariant insulating Hamiltonian H_0 and the second is a disorder potential V_ω. In 2D, H_0 can display topological properties, manifested in the emergence of chiral edge modes. The number of stable chiral edge modes is equal to the C number of the occupied bulk states [21]. By definition, a CI is an insulator with $C \neq 0$. Its *bulk* states display a spectacular behavior, manifested in the persistence of extended states even when the disorder is on. The interesting physics of the CIs is due to these states—the edge modes are nothing but the delocalized bulk states terminating at the edge.

In our calculations, we use the spin-up component of the Kane-Mele Hamiltonian [2] with $\lambda_R = 0$ and $\lambda_{\mathrm{SO}} = \eta - it$ (in order to connect with previous studies [10]):

$$H_0 = \sum_{\langle xy\rangle} |x\rangle\langle y| + \sum_{\langle\langle xy\rangle\rangle} \{\zeta_x |x\rangle\langle y| + \zeta_x^* |y\rangle\langle x|\},$$

where $\zeta_x = \frac{1}{2}\alpha_x(t + i\eta)$ with $\alpha_x =$ the isospin of the site and x, y are sites of a honeycomb lattice. This H_0 displays a topological phase for $|\eta| > |t| \tan\frac{\pi}{6}$. For disorder we use uniform random entries $\omega_x \in [-\frac{1}{2}, \frac{1}{2}]$.

We first use the traditional level statistics analysis of the EnS to probe the extended or localized character of the bulk states. Figure 1 shows the EnS of H_ω at disorder strengths $W = 3$, 5, 8, and 11, when H_0 is in topological [Fig. 1(a)] and trivial [Fig. 1(b)] phases. The energy levels are shown on the vertical axis for 10^3 disorder configurations offset horizontally. Overlaid is the variance of the energy level spacings, collected at all energies using a small window. From the histograms, we see two regions where the level-spacing distribution perfectly matches the Wigner-Dyson distribution $P_{\mathrm{GUE}}(s) = \frac{32s^2}{\pi^2} e^{-4s^2/\pi}$. The level-spacing variance $\langle s^2\rangle - \langle s\rangle^2$ at these energies converges to the variance of $P_{\mathrm{GUE}} \simeq 0.178$. We infer that these regions of level repulsion contain extended states. In the rest of the spectrum, the histograms match the Poisson distribution $P_P(s) = e^{-s}$ and the variance takes large values [$O(1)$]. We infer that in these regions the states are localized. Upon increasing W, the regions of delocalized spectrum (where the variance is exactly 0.178) converge towards each other to eventually collide and disappear. This is consistent with the "levitation and annihilation" phenomenon [10] and suggests the phase diagram shown in Fig. 1(a). In contrast, if we start from the normal insulator and increase W, all the states localize [see Fig. 1(b)] at any disorder strength and there is no diffusive regime [a small variance in Fig. 1(b) (a) is a finite size effect [22]].

We corroborate these results with a calculation of the Chern number C. For a clean system,

$$C = \frac{1}{2\pi i} \int_{\mathrm{BZ}} \mathrm{tr}\{\hat{P}(k)[\partial_{k_1}\hat{P}(k), \partial_{k_2}\hat{P}(k)]\} d^2k, \qquad (1)$$

where $\hat{P}(k)$ is the k decomposition of the projector P onto the occupied states. In real space,

$$C = 2\pi i \sum_\alpha \langle 0, \alpha | P[-i[\hat{x}_1, P], -i[\hat{x}_2, P]] | 0, \alpha\rangle. \qquad (2)$$

Equation (2) is useful, as it allows one to treat finite disorder. A classic result [23] states that the disorder average $-2\pi i\langle\sum_\alpha \langle 0, \alpha | P_\omega[[\hat{x}_1, P_\omega], [\hat{x}_2, P_\omega]] | 0, \alpha\rangle\rangle_\omega$, ($P_\omega =$ the projector onto the occupied states of H_ω) is an integer if E_F is in a region of localized EnS. This integer can change its value *only* if E_F crosses a region of extended states, a property that allows one to map the delocalized spectrum. Moreover, if H_0 and E_F are chosen such that $C \neq 0$ at $W = 0$, then moving in any direction in the (E_F, W) plane from that initial point, C will eventually become zero for one of the following reasons: (1) $P_\omega = 0$ if E_F is very negative, (2) $P_\omega = 1$ if E_F is very positive, or (3) all the states localize if W is too large. This implies the existence of a region of extended states surrounding the CI phase and explains the phase diagram of Fig. 1.

Unfortunately, Eq. (2) only makes sense in the thermodynamic limit. We derive a finite size real-space formula for C that converges exponentially fast to the thermodynamic limit. It does not involve twisted boundary conditions, which not only eliminates the problems associated with level crossings at E_F, but allows us to compute C for large systems and many disordered configurations. Additionally, our formula for C requires only knowledge of the ground state.

For clean CIs, C is computed using a discretized Brillouin-zone: $k_n = n_1\Delta_1 + n_2\Delta_2$, $n_{1,2} = 1, \ldots, N$, $|\Delta_i| = \Delta = \frac{2\pi}{N}$. The partial derivatives $\partial_{k_i}\hat{P}$ are replaced by finite differences $\delta_i\hat{P}(k_n) = \sum_m c_m \hat{P}(k_n + m\Delta_i)$ and the integration by a Riemann sum. Because the integrand in Eq. (1) is a periodic and analytic function, with an appropriate choice for the $\delta_i\hat{P}(k_n)$ approximation, the discretized formula converges exponentially fast to the

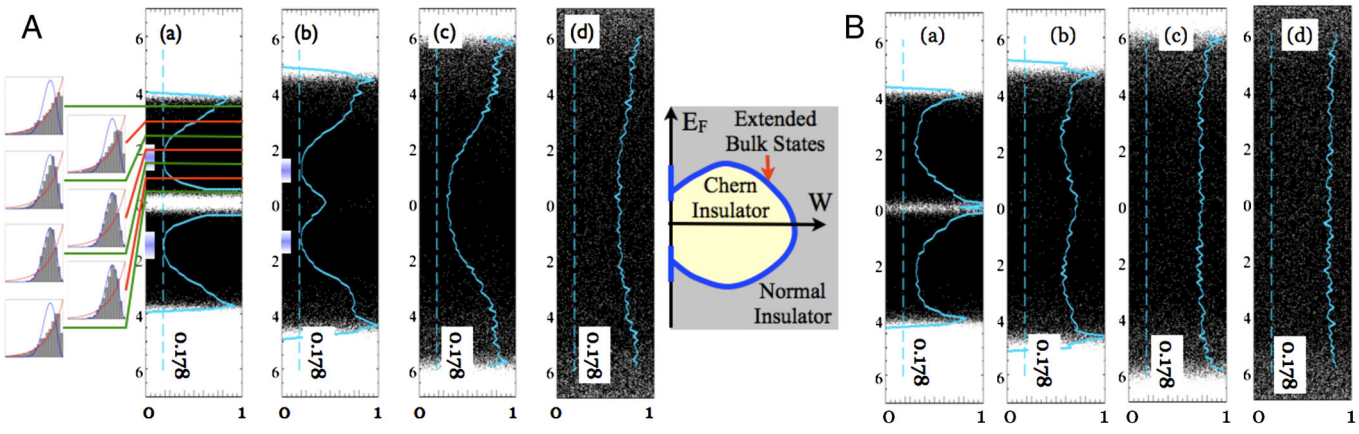

FIG. 1 (color online). EnS and level statistics for a disordered (A) CI ($\zeta = 0.3i$) and (B) trivial insulator ($\zeta = 0.3$), at disorder strengths $W =$ (a) 3, (b) 5, (c) 8, and (d) 11. Panel (A) also shows the phase diagram of the disordered CI inferred from panels (a)–(d), and a few histograms of the level spacings recorded at the indicated energies. The histograms are compared with $P_{\mathrm{GUE}}(s)$ [light grey (blue) line] and $P_{\mathrm{Poisson}}(s)$ [grey (red) lines] distributions. The light grey (blue) lines overlaying the EnS are the variances of the energy-spacing distributions plotted on a scale between 0 and 1. The dashed light grey (blue) line represents the variance (~ 0.178) of P_{GUE}.

continuum limit. To obtain our real-space representation, we note that the discretized C formula can be written as $-i\,\mathrm{Tr}\{P[\delta_1 P, \delta_2 P]\}$, where the trace is over the whole Bloch basis $|\boldsymbol{k}_n\alpha\rangle$ and P is the full projector: $P = \sum_n |\boldsymbol{k}_n\alpha\rangle P_{\alpha\beta}(\boldsymbol{k}_n)\langle\boldsymbol{k}_n\beta|$. Since the trace is invariant to a change of basis, we express this trace in the dual real-space basis $|\boldsymbol{x}, \alpha\rangle$. The result is similar to that of Eq. (2) but with the substitution ($c_m = -c_{-m}$)

$$-i[\hat{x}_i, P] \to \sum_m c_m e^{-im\boldsymbol{\Delta}_i\hat{\boldsymbol{x}}} P e^{im\boldsymbol{\Delta}_i\hat{\boldsymbol{x}}}. \tag{3}$$

If c_m's are chosen so that $x - \sum_{m=-N/2}^{N/2} c_m e^{imx\Delta} = O(\Delta^N)$, the above substitution leads to exponentially small $O(\Delta^N)$ errors. Together with the localization of P, this leads to an exponentially fast converging formula.

For a clean CI ($\zeta = 0.3i$), the formula gives $C = 0.999\,999\,8/0.999\,999\,998$ for a $30 \times 30/40 \times 40$ lattice. The values at $W = 3$ are shown in Fig. 2(a). These calculations were performed for the 30×30 and 40×40 lattices, 10^3 configurations and for seven E_F values. The disorder averaged C values (for the 40×40 lattice) are 0.9999, 0.998, 0.85, 0.53, 0.17, 0.01, and 0.0001 for $E_F = 0$, 0.5, 1.0, 1.5, 2.0, 2.5, and 3.0, respectively. These values indicate the existence of a delocalized spectral region between $E = 1.0$ and 2.0, in good agreement with Fig. 1(a). The topological character of the CI survives disorder.

We now ask if the topological character of a CI has a clear signature in the EtS of the state. We compute the reduced density matrix by cutting a torus-shaped sample in two equal parts A and B, and then tracing out B. The system is noninteracting, so we can use the single-particle EtS. This involves [24] finding the eigenvalues ξ_m of the one-particle correlation function $C_{\boldsymbol{xy}} = \langle c_{\boldsymbol{x}}^\dagger c_{\boldsymbol{y}}\rangle$, where $\boldsymbol{x}$, $\boldsymbol{y}$ are lattice sites of the section that is not traced out, and the expectation value is taken in the ground state of the system. The reduced density matrix can be decomposed in normal modes with energies related to ξ_m, $\rho_A \sim e^{-\sum_m \epsilon_m a_m^\dagger a_m}$ with $\epsilon_m = \frac{1}{2}\log(\frac{1-\xi_m}{\xi_m})$ where a_k are normal mode operators. The ϵ_m's are "entanglement energies." In the clean limit, we perform translationally invariant cuts and plot ξ_m's as function of momentum along the cut, as in Fig. 3(a). When E_F is in the bulk gap, the ξ_m's are primarily concentrated around 0, 1 and have little dispersion. These are either bulk states deep in region A ($\xi_m \sim 1$), or deep in region B ($\xi_m \sim$). We call the difference between the levels at $\xi = 1$ and the ones at $\xi = 0$ the entanglement bulk gap. For a trivial insulator, this is the whole story. For a nontrivial insulator as in Fig. 3(a), an entanglement mode localized on the cut crosses the entanglement bulk gap, much like an edge state in the EnS. As such, the EtS can differentiate between a topological and a trivial insulator, even though we are looking *only* at the bulk ground state wave function for a system *without* boundaries.

We now add disorder. Unfortunately, when E_F is at half filing, the number of the ξ_m levels that are away from 0 or 1 (i.e., the entanglement "edge spectrum") is very small. As such, the large spacings between these levels render them in the clean regime of a random matrix. These "entanglement edge" levels exhibit strong level repulsion as can be clearly seen by the naked eye in Fig. 3(b). The disorder mixing of these levels is small (unless we go to high disorder where the CI is destroyed) and the level-spacing variance, although small, differs from 0.178. A computation with a larger 40×40 lattice shows a decrease of the variance. This is consistent with results in the almost clean

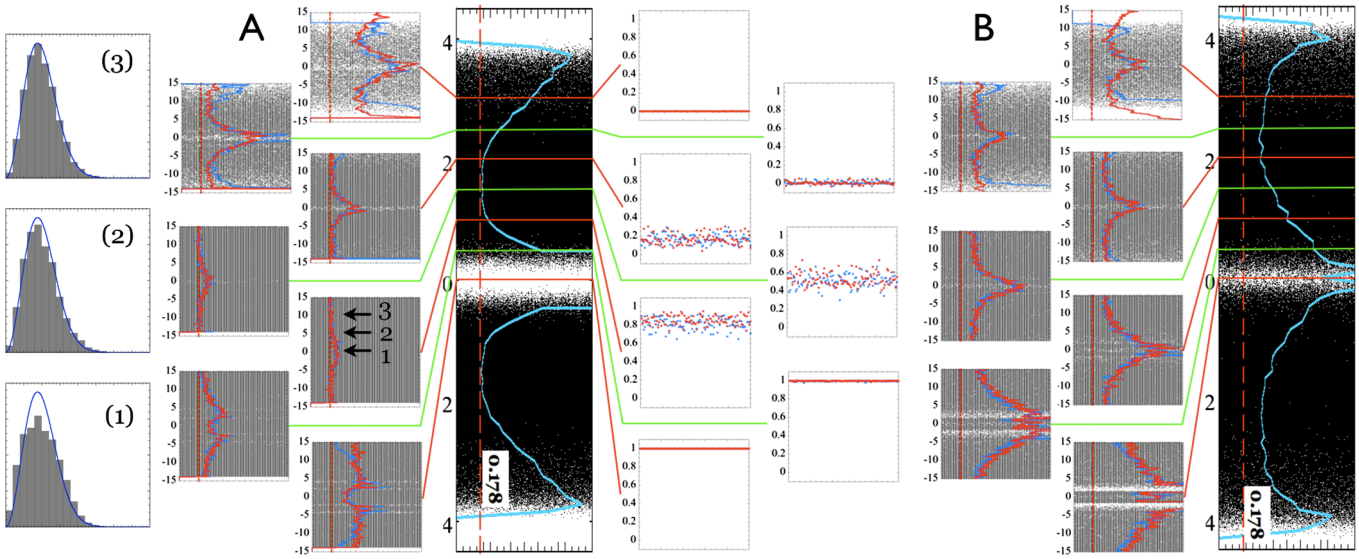

FIG. 2 (color online). (A) EtS and the variance of the level spacings (left panels), EnS (center panel) and C number (right panels) for (A) $\zeta = 0.3i$ CI and (B) $\zeta = 0.3$ normal insulator both with $W = 3$. The EtS and C were computed for seven E_F's as indicated. The light grey and grey (blue and red) data correspond to calculations on $30 \times 30/40 \times 40$ lattices. C was identically zero for the normal insulator. The vertical dotted line in the EtS plots marks the 0.178 value. Panels (1–3) show the histograms of the level spacings collected at the entanglement energies marked by arrows. Overlaid is the Wigner-Dyson distribution $P_{\mathrm{GUE}}(s)$.

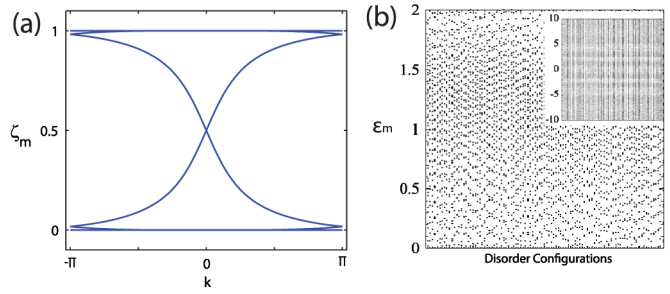

FIG. 3 (color online). (a) Entanglement spectrum for a translationally invariant CI plotted versus momentum along the cut. (b) Level repulsion of the edge entanglement spectrum with disorder. Inset shows the full EtS.

limit of the EnS, where the disorder energy perturbation of each state is smaller than the mean level spacing [22]. These levels exhibit level repulsion and are delocalized.

We now shift E_F and recompute the EtS and the variance of its level spacings. The results are shown in Fig. 2 for $W = 3$. As we move E_F towards the delocalized EnS, we notice that the level statistics of the EtS (in ϵ_m) acquires an increasingly flat region of level spacings displaying a variance of 0.178. As the E_F is moved up from half filling, the EtS becomes more and more diffusive (i.e., departs from the clean limit of the half-filled finite-size problem). Delocalized bulk levels (which are at large negative or positive ϵ) start moving in. When E_F sits right on top of the delocalized EnS, the *whole* EtS becomes delocalized and has variance extremely close to the Wigner-Dyson surmise of 0.178. The histograms of the level spacings collected from small windows at three widely spaced entanglement energies show well-defined distributions matching closely the $P_{\mathrm{GUE}}(s)$. The observation of this delocalization plateau in the EtS corresponding to the ground state of the system filled up to the extended state energy is our main result. As E_F is moved above the extended states and into the region of the trivial Anderson insulator, the entanglement spectrum starts to become localized, with the spectrum near the center starting first. In contrast, for a trivial insulator, the EtS never has regions of level repulsion for any EtS of any ground state. The calculations in Fig. 2 were performed for 30×30 and 40×40 lattices which give similar results, although with reduced noise for the latter.

The behavior of the EtS can be understood by noticing that C_{xy} is identical to the projection operator onto the occupied states, which can be regarded as a flat-band Hamiltonian. EtS is then *identical* to the spectrum of this flat-band Hamiltonian *with open* boundary conditions (BC) at the edge of the untraced region. The periodic BC flat band Hamiltonian has eigenvalues at 0 and 1, and the open BC Hamiltonian will have most of its eigenvalues close to 0 or 1 as well. If the original system was an insulator, then the eigenvalues between 0 and 1 are separated by an entanglement gap, but if topologically nontrivial, the spectrum also has edge modes crossing the entanglement gap. This is an inescapable conclusion that requires no calculation. The projector onto occupied states satisfies the same symmetries as the original Hamiltonian. The projector Hamiltonian has long-range hoppings when E_F is at the mobility edge, and we conjecture that this results in the flat, delocalized behavior of the *full* EtS.

In conclusion, the EnS, EtS, and a new finite-size Chern number formula in the presence of strong disorder yield matching results and can be used to characterize the CI to Anderson-insulator transition. We found that all the levels of the EtS of a CI ground state filled up to the edge of the mobility gap exhibit level repulsion consistent with the Wigner-Dyson distribution (the many-body EtS matrices belong, however, to Wishart ensembles rather than Unitary ones). This delocalized plateau in the entanglement spectrum could be used to gain information about the many-body localization problem.

B. A. B. was supported by Princeton Startup Funds, the Alfred P. Sloan Foundation, and NSF Grant No. DMR-095242, and thanks the Institute for International Collaboration in Beijing for generous hosting. T. L. H. was supported in part by the NSF Grant No. DMR 0758462 at the University of Illinois, and by the ICMT. E. P. acknowledges support from the Research Corporation for Science Advancement.

[1] F. D. M. Haldane, Phys. Rev. Lett. **61**, 2015 (1988).
[2] C. L. Kane and E. J. Mele, Phys. Rev. Lett. **95**, 226801 (2005).
[3] B. A. Bernevig and S. C. Zhang, Phys. Rev. Lett. **96**, 106802 (2006).
[4] B. A. Bernevig *et al.*, Science **314**, 1757 (2006).
[5] M. Konig *et al.*, Science **318**, 766 (2007).
[6] H. Obuse *et al.*, Phys. Rev. B **78**, 115301 (2008).
[7] K. Nomura, M. Koshino, and S. Ryu, Phys. Rev. Lett. **99**, 146806 (2007).
[8] S. Ryu *et al.*, Phys. Rev. Lett. **99**, 116601 (2007).
[9] A. M. Essin and J. E. Moore, Phys. Rev. B **76**, 165307 (2007).
[10] M. Onoda, Y. Avishai, N. Nagaosa, Phys. Rev. Lett. **98**, 076802 (2007).
[11] D. N. Sheng *et al.*, Phys. Rev. Lett. **97**, 036808 (2006).
[12] H. Li and F. D. M. Haldane, Phys. Rev. Lett. **101**, 010504 (2008).
[13] N. Regnault *et al.*, Phys. Rev. Lett. **103**, 016801 (2009).
[14] R. Thomale *et al.*, Phys. Rev. Lett. **104**, 180502 (2010).
[15] R. Thomale *et al.*, arXiv:0912.0028.
[16] F. D. M. Haldane, in "Proceedings of the APS 2009 March Meeting" (unpublished).
[17] L. Fidkowski, Phys. Rev. Lett. **104**, 130502 (2010).
[18] A. M. Turner *et al.*, arXiv:0909.3119.
[19] M. Kargarian and G. A. Fiete, arXiv:1005.3815.
[20] M. L. Mehta, *Random Matrices* (Academic, New York, 1991).
[21] E. Prodan, J. Math. Phys. (N.Y.) **50**, 083517 (2009).
[22] E. Cuevas *et al.*, J. Phys. Condens. Matter **10**, 295 (1998).
[23] J. Bellissard *et al.*, J. Math. Phys. (N.Y.) **35**, 5373 (1994).
[24] I. Peschel, J. Stat. Mech. (2004) P06004.